Analysis of seismic anisotropy parameters for sedimentary strata

Fuyong Yan[1], De-hua Han[1], Samik Sil[2], and Xue-Lian Chen[3], [1]University of Houston, Texas, [2]Occidental Petroleum, Texas, [3]China University of Petroleum*

Summary

Based on a large quantity of laboratory ultrasonic measurement data of sedimentary rocks and using Monte Carlo simulation and Backus averaging, the layering effects on seismic anisotropy are analyzed. The layering effects are studied for different types of rocks under different saturation conditions. If the sedimentary strata consist of only isotropic sedimentary layers and are brine saturated, the δ value for the effective transversely isotropic (TI) medium is usually negative. However, the δ value will increase for gas bearing strata. Based on simulation results, c_{13} can almost perfectly be determined by other TI elastic constants for a layered medium consisting of isotropic layers. Therefore, δ can be predicted from the other Thomsen parameters with confidence. The anisotropic properties of the interbedding system of shales and isotropic sedimentary rocks are primarily controlled by the intrinsic anisotropy of shales. There are fair correlations among the Thomson anisotropy parameters.

Introduction

At various scales, the earth and the subsurface are often modeled as layered sequence of different constituents. Sedimentary strata are layered sedimentary rocks. Observed from the outcrops and seismic profiles, the most prominent feature of sedimentary basins is often the layered structure. The elastic properties of a layered medium can be described by transverse anisotropy (Postma, 1955; Anderson, 1961; Backus, 1962; Helbig, 1984).

The effective anisotropic properties of two periodically alternating isotropic layers are described by Postma (1955). Backus (1962) extended the model to any combination of layers with either isotropic or transversely isotropic (TI) properties. Schoenberg and Muir (1989) further extended the Backus model to more general cases that the constituent layers can be any type of anisotropic media. From the wireline logging data, the lithology or acoustic property variations of the sedimentary layers are often in scale of decimeters, whereas the wavelength of the seismic waves are usually in the order of 100 meters. Therefore, the effective media through which the seismic waves propagate are usually, more or less, anisotropic. Study of the effective anisotropic properties of the layered media is important for seismic exploration.

Based on Backus averaging and Monte Carlo simulation of 2- and 3-layer cake models, Berryman (1999) analyzed the relationships among the Thomsen parameters. The study showed little indication of the correlations between the anisotropy parameters except for the possible range and sign of the parameters. The simulation results were not very helpful for understanding the seismic anisotropic properties of sedimentary rocks. In this study, a more realistic study will be performed using similar approaches by Berryman (1999), but the Monte Carlo simulation will be based on a large quantity of laboratory measurement data of sedimentary rocks. More constituent layers with either isotropic or transversely anisotropic properties are included to simulate the complexity of sedimentary strata.

Monte Carlo Simulation of Sedimentary Strata

The simulation is based on a large amount of laboratory ultrasonic measurement data of various sedimentary rocks. The sandstone data come from Han (1986). The sandstone samples in Han's dataset include typical sandstones coming from various places all over the world. The samples have various clay content. They are measured at both dry and fully brine-saturated states and various pressure conditions. The carbonate rocks come from Rafavich et al. (1984), Kenter et al. (1997), Woodside et al. (1998), Assefa et al. (2003), and Fabricius et al. (2008). The carbonate samples in datasets by Rafavich et al. (1984), Assefa et al. (2003) and Fabricious et al. (2008) are measured on both dry and fully brine-saturated states. The shale data come from Thomsen (1986), Johnston and Christensen (1995), Vernik and Liu (1997), Jakobsen and Johansen (2000), Wang (2002, shale and coal samples only), and Sone (2012, 2013). The saturation conditions of shales are complicated and not classified for analysis. The data points for the dry sandstones are 420, for wet sandstones are 420, for dry carbonates are 144, for wet carbonates are 298 and for shales are 137. Figure 1 shows the probability density functions of α_0 and the ratio of α_0^2/β_0^2 of the experimental data of different types of sedimentary rocks. Here α_0 and β_0 are the vertical P-wave velocity and S-wave velocity, respectively. The dry sandstone and wet sandstone are treated as different classifications of rocks because the effect of saturation on seismic anisotropy parameters is to be studied. It can be seen that different classifications of rocks have different distributions of α_0 and the ratios of α_0^2/β_0^2.

In our study, sedimentary strata are simulated by first randomly selecting a certain number of samples from a

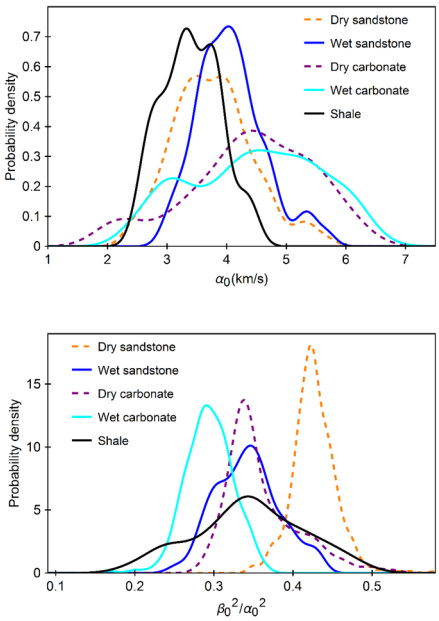

Figure 1: densities of α_0 and β_0^2/α_0^2 of the laboratory data used in this study.

classification of rocks or a combination of classifications of rocks, and then the experimental data of the selected samples are used to parameterize the layer cake model. The elastic properties of each layer in the layer cake model is based on laboratory measurement, not on random sampling in certain ranges that may lose the physical relations between the elastic parameters for the real sedimentary rocks. This is the basic difference between our study and the study by Berryman (1999). Considering the size of the database and the number of simulations, a 15-layer cake model is used. Compared to the 2- or 3-layer cake model, the 15-layer cake model may be more proper to simulate the complex subsurface conditions.

Layering Effect on Seismic Anisotropy in Sedimentary Strata of a Single Lithology

Due to mild depositional environment changes, for the same type of rocks, the mineral composition and texture variation may also cause noticeable acoustic velocity change. The layering effect on seismic anisotropy may be different for different classifications of rocks.

Figures 2 and 3 show the simulation results of the layering effect on seismic anisotropy. In Figure 2, for all the classifications of rocks, the ratio α_0^2/β_0^2 has noticeable effect on δ value. Here the gray data points are for the stratified shale formation with each layer assumed isotropic with the vertical properties. For the layered model of wet sandstones, wet carbonates or isotropy-assumed shales, the δ values are usually negative. Gas saturation has an effect of increasing the δ value. After considering the intrinsic anisotropic properties of the shale layers, the δ values are usually positive.

Figure 3 shows the correlation between ε and γ. The relations between the P-wave anisotropy and S-wave anisotropy are different for different classifications of sedimentary rocks. Generally, the S-wave anisotropy is stronger than the P-wave anisotropy except for the gas-bearing carbonate layers. The ratio of S-wave to P-wave anisotropy will decrease due to the gas saturation effect. Quite different from Berryman's (1999) study, negative values of ε are not observed from 25,000 simulations. It is generally observed and accepted that the seismic velocity is greater along the bedding than in the perpendicular direction if the effect of fractures is not considered. Therefore, the simulation results in this study may be more realistic.

Prediction of δ for Sedimentary Strata Consisting of Isotropic Layers

A TI medium is defined by five elastic constants: c_{11}, c_{33}, c_{44}, c_{66}, and c_{13}. The physical meanings of c_{11}, c_{33}, c_{44} and c_{66} are straightforward and they can usually be reliably determined. In spite of a large amount of experimental studies, the physical meaning of c_{13} is not obvious and its relation with the other TI elastic constants is not clear. This may be due to significant uncertainties in the laboratory determination of c_{13} (Yan et al., 2012, 2013, 2014; Yan, 2015; Yan, et al., 2016). Another approach to study the relations among the TI elastic constants is by numerical simulations.

Based on previous simulation results, Figure 4 shows the correlation between c_{13} and other TI elastic constants. It can be seen that c_{13} can almost be perfectly predicted by other TI elastic constants. The correlation formula is

$$c_{13B} = -0.048 + 0.48\, c_{11B} + 0.46\, c_{33B} - 0.53\, c_{44B} - 1.27\, c_{66B}. \quad (1)$$

The elastic constants are all in GPa, and the regression coefficient is 0.999 based on 20,000 simulations. Considering the different elastic properties between sandstones and carbonates, dry rocks and wet rocks, the quality of this correlation is out of expectation. This means that the elastic properties of a TI medium consisting of isotropic layers can be determined by four independent elastic constants (and not five as for a general TI medium). Equation (1) can be reformulated to predict δ from other Thomsen parameters (Yan, 2015). It should be emphasized

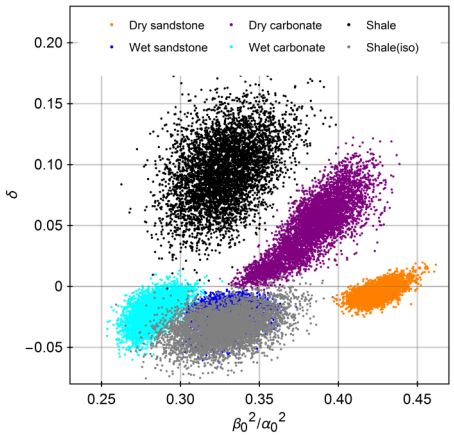

Figure 2: Crossplot between δ and β_0^2/α_0^2. δ and β_0^2/α_0^2 are computed from the Backus averaging of a 15-layer cake model randomly parameterized by the laboratory measurement data. Each cloud of points are from 5000 simulations. For the gray data points, the shale layer is assumed isotropic with the vertical properties.

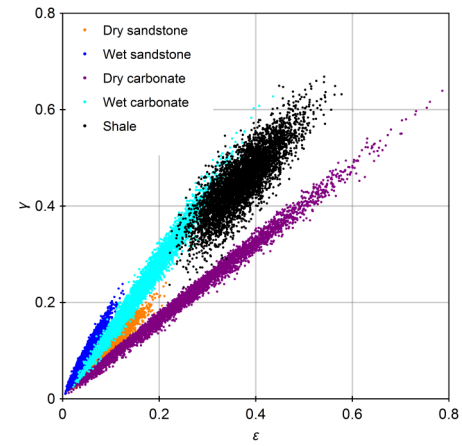

Figure 3: Crossplot between ε and γ. ε and γ are computed from Backus averaging of a 15-layer cake model randomly parameterized by the laboratory measurement data.

that equation (1) only works for sedimentary strata consisting of isotropic layers.

From the Backus averaging scheme, the Thomsen parameter δ for a layered medium can be represented by

$$\delta = 2\left(\frac{\langle c_{44}^{-1}\rangle^{-1}}{\langle c_{33}^{-1}\rangle^{-1}} - \left\langle\frac{c44}{c33}\right\rangle\right)\frac{1-\left\langle\frac{c44}{c33}\right\rangle}{1-\frac{\langle c_{44}^{-1}\rangle^{-1}}{\langle c_{33}^{-1}\rangle^{-1}}}. \qquad (2)$$

Here $\langle * \rangle$ is a volume-averaging operator.

From Monte Carlo simulation of sedimentary strata consisting of isotropic layers, the ratio of $\left(1-\left\langle\frac{c44}{c33}\right\rangle\right)$ to $\left(1-\frac{\langle c_{44}^{-1}\rangle^{-1}}{\langle c_{33}^{-1}\rangle^{-1}}\right)$ is generally very close to one (Yan, 2015). Therefore, for sedimentary strata consisting of isotropic layers, equation (2) can be simplified into

$$\delta \approx 2\left(\frac{\langle c44^{-1}\rangle^{-1}}{\langle c33^{-1}\rangle^{-1}} - \left\langle\frac{c44}{c33}\right\rangle\right). \qquad (3)$$

Figure 5 shows a comparison between δ calculated by the Backus averaging (equation (2)) and δ approximated by equation (3) based on Monte Carlo Simulation of sedimentary strata consisting of isotropic layers. The difference between the theoretical δ value and the approximated δ value is only noticeable at extremely low and high δ values.

Layering Effect on Seismic Anisotropy for Sedimentary Strata of Mixed Lithologies

Except of mild acoustic property change caused by the mineral composition and texture variation for the same type of sedimentary rocks, stronger acoustic property change in a sedimentary formation can be caused by a drastically depositional environment change leading to a lithology change. For example, the interbedding of shales with sandstones and interbedding of shales with carbonate rocks are often-occurring geological scenarios. To model the interbedding effect on seismic anisotropy, the 15-layer cake model is randomly parameterized by the experimental database of shales and one classification of the isotropic rocks.

Figures 6 and 7 show the simulation results of the interbedding effect on seismic anisotropy parameters. Comparing them to Figures 2 to 3, if we know the layering effect on seismic anisotropy for each classification of the sedimentary rocks, the interbedding effect by two classifications of sedimentary rocks on seismic anisotropy is generally predictable. In Figure 6, when the intrinsic anisotropy of shales is considered, the δ values are mostly positive. From Figure 7 there is a good correlation between ε and γ. Shales are a type of rock with complicated mineral composition including clay minerals, quartz and carbonate and organic materials. The interbedding effect on seismic anisotropy is in general consistent with the laboratory studies on shales (Sayers, 2005; Sondergeld and Chandra, 2011). Since the Monte Carlo simulation is based on the experimental data of real sedimentary rocks, the simulation results on the relationships among the seismic anisotropy parameters are quite different from those by Berryman's (1999) study.

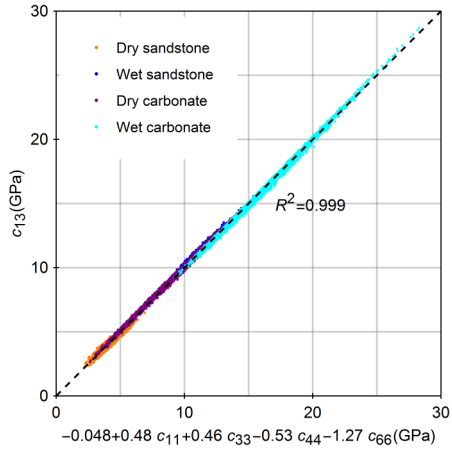

Figure 4: Relation between c_{13} and other TI elastic constants based on Backus averaging of randomly selected 15-layer cake model. 5000 simulations are run for each type of rocks.

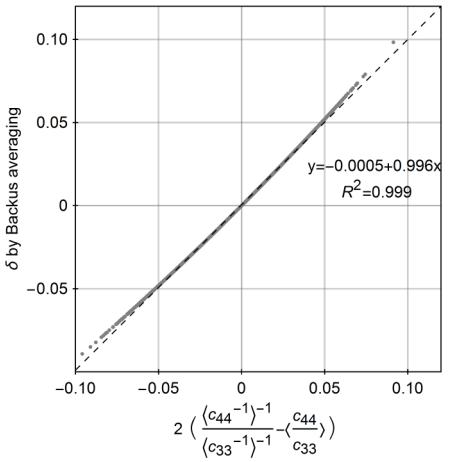

Figure 5: Prediction of δ by $2(\frac{\langle c_{44}^{-1}\rangle^{-1}}{\langle c_{33}^{-1}\rangle^{-1}}-\langle\frac{c_{44}}{c_{33}}\rangle)$ based on a 15-layer cake model randomly selected from the laboratory data of dry or wet sandstone and dry or wet carbonate. Totally 5000 simulations are run.

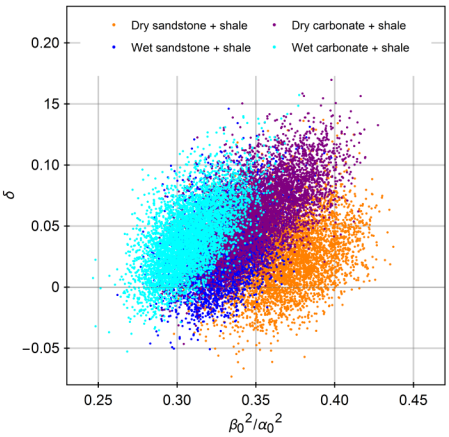

Figure 6: Crossplot between δ and β_0^2/α_0^2. δ and β_0^2/α_0^2 are computed from Backus averaging of 15-layer cake model randomly parameterized by the laboratory measurement data. Each cloud of points are from 5000 simulations. Different colors represent mixture of shale with different classifications of rocks.

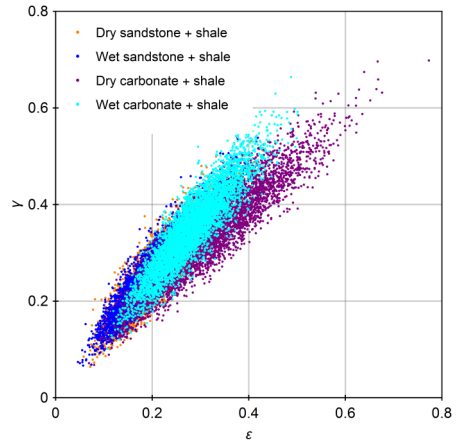

Figure 7: Crossplot between ε and γ. ε and γ are computed from Backus averaging of 15-layer cake model randomly parameterized by the laboratory measurement data.

Conclusions

Based on Backus averaging and Monte Carlo simulation, it is found that the δ value for the sedimentary strata consisting of isotropic wet sandstones or carbonates is usually negative and the gas-bearing thin beds have effect of increasing the δ value. For sedimentary strata consisting of isotropic layers, c_{13} can be determined by other TI elastic constants and δ can be predicted from the other Thomsen parameters with confidence. The anisotropic properties of the interbedding system of shales and isotropic sedimentary rocks are primarily controlled by the intrinsic anisotropy of shales. There are fair correlations among the Thomson anisotropy parameters.

Acknowledgements

We would like to thank the Fluid/DHI consortium sponsors for the financial support.

EDITED REFERENCES

Note: This reference list is a copyedited version of the reference list submitted by the author. Reference lists for the 2016 SEG Technical Program Expanded Abstracts have been copyedited so that references provided with the online metadata for each paper will achieve a high degree of linking to cited sources that appear on the Web.

REFERENCES

Anderson, D. L., 1961, Elastic wave propagation in layered anisotropic media: Journal of Geophysical Research, **66**, 2953–2963, http://dx.doi.org/10.1029/JZ066i009p02953.

Assefa, S., C. McCann, and J. Sothcott, 2003, Velocities of compressional and shear waves in limestones: Geophysical Prospecting, **51**, 1–13, http://dx.doi.org/10.1046/j.1365-2478.2003.00349.x.

Backus, G. E., 1962, Long-wave elastic anisotropy produced by horizontal layering: Journal of Geophysical Research, **67**, 4427–4440, http://dx.doi.org/10.1029/JZ067i011p04427.

Berryman, J. G., V. Y. Grechka, and P. A. Berge, 1999, Analysis of Thomsen parameters for finely layered VTI media: Geophysical Prospecting, **47**, 959–978, http://dx.doi.org/10.1046/j.1365-2478.1999.00163.x.

Fabricius, I., L. Gommesen, A. Krogsboll, and D. Olsen, 2008, Chalk porosity and sonic velocity versus burial depth: Influence of fluid pressure, hydrocarbons, and mineralogy: The American Association of Petroleum Geologists Bulletin, **92**, 201–223, http://dx.doi.org/10.1306/10170707077.

Grotzinger, J., and T. H. Jordan, 2010, Understanding earth, 6th ed.: W.H. Freeman.

Han, D.-H., 1986, Effects of porosity and clay content on acoustic properties of sandstones and consolidated sediments: Ph.D. thesis, Stanford University.

Helbig, K., 1984, Anisotropy and dispersion in periodically layered media: Geophysics, **49**, 364–373, http://dx.doi.org/10.1190/1.1441672.

Jakobsen, M., and T. A. Johansen, 2000, Anisotropic approximation for mudrocks: A seismic laboratory study: Geophysics, **65**, 1711–1725, http://dx.doi.org/10.1190/1.1444856.

Johnston, J. E., and N. I. Christensen, 1995, Seismic anisotropy of shales: Journal of Geophysical Research, **100**, 5991–6003, http://dx.doi.org/10.1029/95JB00031.

Kenter, J., F. Podladchikov, M. Reinders, S. van der Gaast, B. Fouke, and M. Sonnenfeld, 1997, Parameters controlling sonic velocities in a mixed carbonate–siliciclastic Permian shelf-margin (upper San Andres Formation, Last Chance Canyon, New Mexico): Geophysics, **62**, 505–520, http://dx.doi.org/10.1190/1.1444161.

Postma, G. W., 1955, Wave propagation in a stratified medium: Geophysics, **20**, 780–806, http://dx.doi.org/10.1190/1.1438187.

Rafavich, F., C. Kendall, and T. Todd, 1984, The relationship between acoustic properties and the petrographic character of carbonate rocks: Geophysics, **49**, 1622–1636, http://dx.doi.org/10.1190/1.1441570.

Sayers, C. M., 2005, Seismic anisotropy of shales: Geophysical Prospecting, **53**, 667–676, http://dx.doi.org/10.1111/j.1365-2478.2005.00495.x.

Schoenberg, M., and F. Muir, 1989, A calculus for finely layered anisotropic media: Geophysics, **54**, 581–589, http://dx.doi.org/10.1190/1.1442685.

Sondergeld, C. H., and S. R. Chandra, 2011, Elastic anisotropy of shales: The Leading Edge, **30**, 324–331, http://dx.doi.org/10.1190/1.3567264.

Sone, H., 2012, Mechanical properties of shale gas reservoir rocks and its relation to in-situ stress variation observed in shale gas reservoirs: Ph.D. thesis, Stanford University.

Thomsen, L., 1986, Weak elastic anisotropy: Geophysics, **51**, 1954–1966, http://dx.doi.org/10.1190/1.1442051.

Vernik, L., and X. Liu, 1997, Velocity anisotropy in shales: A petrophysical study: Geophysics, **62**, 521–532, http://dx.doi.org/10.1190/1.1444162.
Wang, Z., 2002, Seismic anisotropy in sedimentary rocks, part 2: Laboratory data: Geophysics, **67**, 1423–1440, http://dx.doi.org/10.1190/1.1512743.
Woodside, J., J. Kenter, and A. Köhnen, 1998, Acoustic properties from logs and discrete measurements (sites 966 and 967) on Eratosthenes Seamount: Controls and ground truth: Proceedings of the Ocean Drilling Program. Scientific Results, **160**, 535–543.
Yan, F., 2015, Analysis of anisotropy parameters for sedimentary rocks and strata: Ph.D. thesis, University of Houston.
Yan, F., D.-H. Han, and Q. Yao, 2012, Oil shale anisotropy measurement and sensitivity analysis: 82nd Annual International Meeting, SEG, Extended Abstracts, 1–5, http://dx.doi.org/10.1190/segam2012-1106.1.
Yan, F., D.-H. Han, and Q. Yao, 2013, Physical constraints on c_{13} and Thomsen parameter delta for VTI rocks: 83rd Annual International Meeting, SEG, Extended Abstracts, 2889–2894, http://dx.doi.org/10.1190/segam2013-0424.1.
Yan, F., D.-H. Han, and Q. Yao, 2014, Benchtop rotational group velocity measurement on shales: 84th Annual International Meeting, SEG, Extended Abstracts, 2983–2986, http://dx.doi.org/10.1190/segam2014-1569.1.
Yan, F., D.-H. Han, and Q. Yao, 2016, Physical constrains on c_{13} and δ for transversely isotropic hydrocarbon source rocks: Geophysical Prospecting, http://dx.doi.org/10.1111/1365-2478.12265.